Applied Physics B (2020) 126:14
https://doi.org/10.1007/s00340-019-7368-8

Applied Physics B
Lasers and Optics

Suppression of parasitic lasing and inter-pulse self-pulsing in a pulsed Erbium–Ytterbium co-doped fiber amplifier

Lalita Agrawal[1,2] · **Dinesh Ganotra**[2]

Received: 7 July 2019 / Accepted: 9 December 2019 / Published online: 18 December 2019

Abstract
Performance of an Erbium–Ytterbium co-doped fiber (Nufern PM EYDF 12/130) has been investigated as a power amplifier stage for developing a pulsed, high peak power, 1550 nm laser with 30 ns pulse duration at 10 kHz repetition rate. A directly modulated, broadband, Fabry–Perot laser diode has been employed as seed laser in all fiber master oscillator power amplifier (MOPA) configuration. Amplifier performance was significantly improved by improving the spectral quality of seed and preamplifiers using two band-pass filters in tandem. This may be attributed to the reduction in inter-pulse Amplified Spontaneous Emission (ASE) noise. Comparative results have been presented for two different MOPA configurations. MOPA with broader signal spectrum resulted in Yb parasitic lasing at 5 W pump power causing roll over in the output energy. Also, onset of strong self-pulsing was observed during off period (in absence of signal pulse) at ~ 6.3 W input. Nature of these pulses resembled relaxation oscillations. Theoretically calculated time period (10–12 µs) of the self-pulses at various pump powers matched fairly well with the experimental results. However, with improved signal spectral quality, no such inter-pulse self-pulsing and parasitic lasing was observed up to 12 W pump power. More than 75 µJ energy per pulse was achieved, limited by power-handling capability of the output isolator. We present here several novel experimental results in terms of spectral, temporal and energy output for a pulsed EYDF amplifier generating 2.5 kW pulses @ 1550 nm.

1 Introduction

Erbium and Erbium–Ytterbium co-doped fiber (EYDF) lasers/amplifiers, operating in pulsed mode, are rapidly replacing the conventional Q-switched bulk solid-state lasers for generating nano-second pulses at multi-kHz repetition rates. Besides offering advantages of eye safety and high atmospheric transparency, their fully integrated all-fiber structure provides compact, robust, alignment-free, high beam quality laser, suitable for variety of applications. They are very attractive candidates for many long-range applications such as ranging, remote sensing, 3D imaging and LIDAR, etc.

Yb ion is typically added as a sensitizer in Erbium-doped fibers to improve pump absorption, hence EYDF amplifiers are more efficient than pure Erbium fiber amplifiers. But under very strong pumping, bottlenecking effect may arise where the excited Yb ions do not transfer energy quickly to the Er ions, thus promoting the Yb ions to lase. It was first proposed to have controlled simultaneous laser oscillation near 1 µm to increase the power level at 1.5 µm [1]. Since then, several methods are being employed to suppress Yb parasitic lasing, e.g. adding an auxiliary signal from Yb band, which was experimentally [2, 3] and theoretically investigated [4, 5]. In another method, a positive feedback loop for Yb signal was employed [6–8]. All these methods have been criticized in [9] for their complexity and unconfirmed effectiveness in pulsed operation. Authors in [9] have used an all solid-state photonic bandgap fiber for suppression of Yb parasitic lasing in a pulsed EYDF amplifier. But the operating repetition rate is relatively high, i.e. 200 kHz with a pulse width of 100 ns. At such rates, the time for ASE accumulation between the pulses is automatically reduced. Many applications require operation at lower repetition rates (1–10 kHz) such as LIDAR and target illumination, etc. At lower repetition rates, higher inversion can be achieved in the gain medium thus more energy can be extracted than that can be achieved at higher repetition rates. But under CW pumping, the inter-pulse ASE is required to be managed to

✉ Lalita Agrawal
lalitaagrawal@lastec.drdo.in

[1] Laser Science and Technology Centre, Delhi, India

[2] Indira Gandhi Delhi Technical University for Women, Delhi, India

avoid unwanted depletion of inversion before the arrival of signal pulse. Authors in [10] used both active (EOM) and passive techniques (ASE filter), up to third stage, to control the inter-pulse ASE when operating under CW pumping. In our work, we have used only band-pass filters to significantly reduce the inter-pulse ASE. The scheme proposed in [10] is rather involved and number of amplifier stages is also more. The maximum energy obtained was 0.3 mJ for 300 ns and 0.38 mJ for 1000 ns pulse widths, respectively, at 3 kHz from 25/300 EYDF amplifier at 15 W pump power (976 nm). Parameters such as fiber core size and pulse width are different from ours but their third-stage fiber (10/125) is very close to our case (12/130), so we may compare the peak powers of these stages at 10 kHz. We have achieved about 4.5 times more peak power (2.5 kW) than achieved (0.55 kW) in [10].

In present work, we have been able to significantly reduce the inter-pulse ASE and thus self-pulsing and Yb parasitic lasing, by employing two band-pass filters in tandem after broadband seed and preamplifier stages, thus avoiding gating and pulsed pumping up to a pump power of 12 W. We have observed the ASE build-up dynamics in time domain by strongly oversaturating photodetectors as suggested in [11]. But here, we have used both silicon and InGaAs photodetectors to discriminate the Yb signal from Erbium signal.

We also employed off-peak pumping to increase the Yb lasing threshold, as suggested in [12, 13], although could not get much advantage as Yb parasitic lasing was observed near 976 nm instead of 1000–1100 nm spectral range as mentioned in [12, 13]. As the optical spectrum analyser available with us does not cover entire range of 600–1700 nm, we have used two separate optical spectrum analysers for two different ranges (600–1100 nm and 1530–1560 nm) along with a suitable dichroic mirror for spectral analysis.

Self-pulsing in Erbium-doped fiber lasers has been widely reported in CW operation [14–20], it may lead to instabilities and can be detrimental for various components. Such a behavior has been attributed to different mechanisms, e.g. re-absorption of laser photons in un-pumped part of fiber, Erbium ion clustering or ion-pair formation [16, 18], ASE noise [21], back reflections and scattering processes [15, 22], etc. Several methods have been suggested to suppress self-pulsing, e.g. resonant pumping [23], intra-cavity semiconductor optical amplifier (SOA) [24], inserting a low-power laser as an auxiliary pump [25] and using electronic feedback for pumping laser [26], etc. It has also been reported that Yb co-doping supports suppression of self-pulsing [27].

In present work, we have observed self-pulsing in pulsed EYDF amplifier during off period under continuous pumping of the gain fiber. It has been attributed to relaxation oscillation mechanism [14] as the experimental results match fairly well with the theoretical estimations. We have been able to suppress this self-pulsing also along with Yb parasitic lasing as mentioned above.

In short, we present here several novel experimental results in terms of spectral, temporal and energy output for a pulsed EYDF amplifier operating at 30 ns, 10 kHz, generating 2.5 kW pulses @ 1550 nm.

2 Experimental details

Experiments on two different master oscillator power amplifier (MOPA) configurations were performed. A directly modulated, broadband, high peak power (365 mW) Fabry–Perot laser diode with an isolator spliced at its output has been employed as seed laser. Broader spectrum (~8 nm) of seed laser was reduced to ~3 nm using a band-pass filter (BPF) in configuration-I (Fig. 1). As per data sheet, the BPF used in first configuration has central wavelength of 1550 nm with 5.5 nm bandwidth (FWHM). Seed laser diode was operated in pulsed mode (30 ns, 10 kHz) using a customized pulsed laser diode driver which can deliver pulsed currents up to 3 A. Pulsed signal from seed is pre-amplified through ~2 m long single-mode Erbium-doped fiber (Nufern PM ESF 7/125), which is bi-directionally pumped by 976 nm

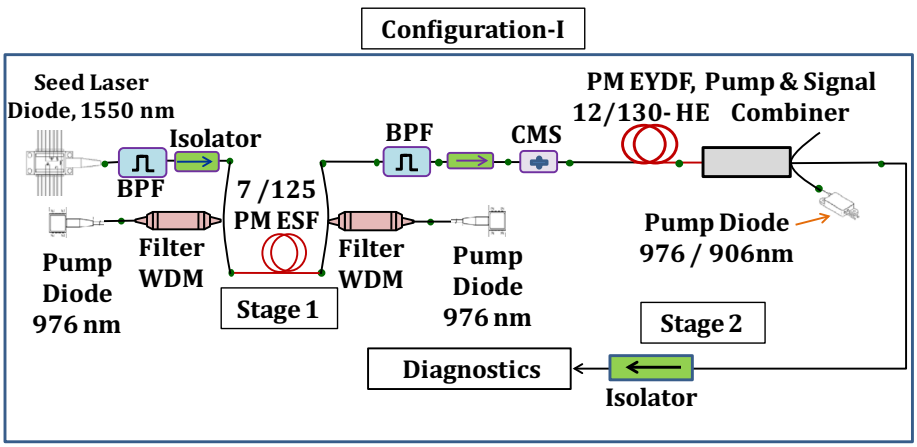

Fig. 1 Schematic of MOPA configuration-I

CW laser diodes (each with 600 mW maximum power). Filter type Wavelength Division Multiplexers (WDMs) have been used to couple pump and signal powers into the fiber. Output from the first amplifier stage goes to a BPF and suitable isolator through the reflected port of backward WDM. Second-stage amplifier is an Erbium–Ytterbium co-doped fiber (Nufern PM EYDF-12/130-HE), backward pumped through a $(2\times1)+1$ pump combiner using conduction cooled 976 nm or 906 nm laser diode, placed on a water-cooled plate, and operated in CW mode. Active fiber length of 1.2 m was used for 976 nm pumping (absorption 8.1 dB/m) while for 906 nm, 3.1 m long fiber was used due to its lower absorption coefficient (2.1 dB/m).

Output spectra were observed in two wavelength bands, i.e. (600–1100 nm) and (1530–1560 nm), using suitable dichroic mirror (Fig. 2). Laser pulses were monitored by both silicon and InGaAs photodetectors placed in close proximity of the output end to capture inter-pulse ASE.

Second configuration, configuration-II (Fig. 3) was realized with two preamplifier stages consisting of Erbium-doped fibers of optimized lengths. Two BPFs (with ~ 2 nm pass band around 1550 nm) after seed and second preamplifier stage have been employed in tandem to increase the loss in rejection band thus reducing the inter-pulse ASE noise. BPFs used in second configuration have central wavelength of 1550 nm with less than 2 nm bandwidth at 0.5 dB and less than 6 nm bandwidth at 25 dB points. To the best of our knowledge, it is a much simpler scheme leading to suppression of self-pulsing and parasitic lasing up to 12 W of pump power (906 nm).

2.1 Fiber length estimation

Fiber lengths in preamplifier stages were optimized by cut back technique. Starting from ~ 4 m long fibers, length was cutback in several small steps to maximize the output energy. To avoid trial and error and wastage of fiber in cutback technique, fiber length for EYDF amplifier stage was chosen for ~ 10 dB pump power absorption. Active fiber length of 1.2 m was used for 976 nm pumping (absorption 8.1 dB/m), while for 906 nm, 5 m long fiber should have been used due to its lower absorption coefficient (2.1 dB/m).

But in pulsed amplifiers due to high peak powers involved, one must take into consideration the non-linear effects such as stimulated Raman scattering (SRS) and stimulated Brillouin scattering (SBS). As our seed has a broader spectral width, SBS effects may be neglected and SRS threshold was estimated as given in [29]

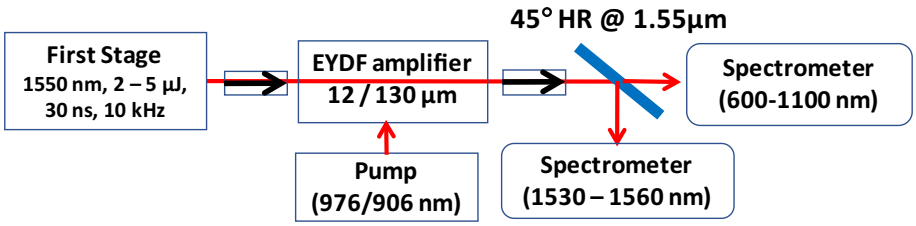

Fig. 2 Schematic for spectral analysis

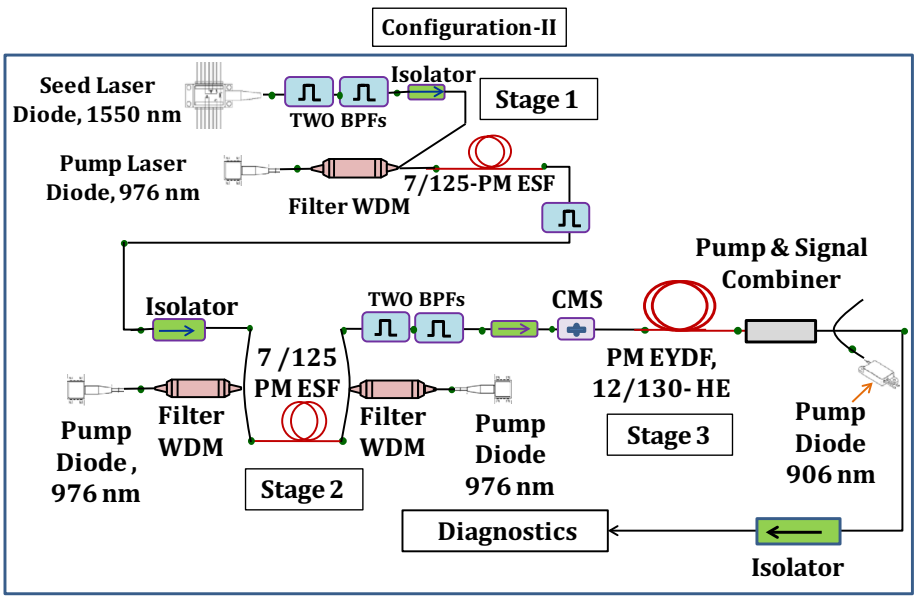

Fig. 3 Schematic of MOPA configuration-II

$$P_{\text{thld}}^{\text{SRS}} = \frac{16 \times \pi \times a^2}{g_{\text{R}} L} \times \Gamma^2 \times \ln(G),$$

where 'a' is the core radius (6 μm in present case), Γ is overlap factor (typical 80%), g_{R} is Raman gain (~ 10^{-13} m/W for silica), G is amplifier gain factor (ratio: output/input) and L is actual fiber length.

Assuming typical gain of about 15 dB (corresponding to $G \sim 30$) for 5 m length, we get

$$P_{\text{thld}}^{\text{SRS}} \sim 7.8\,kW.$$

In configuration-I, for input energy of 5.2 μJ to the amplifier with a gain factor of 30, we expect to get ~ 150 μJ resulting in ~ 5 kW peak power for 30 ns pulse width. Thus, to work well below SRS threshold, we used 3.1 m fiber length. In configuration-II, same length was kept for comparing the results.

3 Results and discussion

Performance of each stage was analyzed experimentally. Output spectra were monitored in two bands (600–1100 nm) and (1530–1560 nm) employing a suitable dichroic mirror and spectrometers, Wavestar (M/s Ophir, Israel) and SHR-IR Wavelength Meter (M/s Solar, Belarus), respectively. Pulse energy was monitored directly using different energy meter (make M/s Ophir, Israel) heads for different amplifier stages. Laser pulses were monitored by both silicon (M/s Thorlabs, USA) and InGaAs photodetectors (1623, NewFocus, USA) placed in close proximity of the output end to capture interpulse ASE.

3.1 Comparative performance results

3.1.1 Spectral profiles

Seed laser spectrum of configuration-I is shown in Fig. 4a, with and without BPF. Spectral quality of seed laser improved considerably using two band-pass filters (Fig. 4b) in configuration-II. Due to insertion of BPFs, output pulse energy at 3 A peak current reduced from 11 nJ (without BPF) to 7 nJ (with single BPF in configuration-I) and 0.8 nJ (with two BPFs in configuration-II) for 30 ns pulses at 10 kHz.

Output spectrum of amplifier stages for both configurations is depicted in Fig. 5a, b. As can be seen the background ASE noise is significantly less in configuration-II even at 12 W pump power @ 906 nm as compared to spectra in configuration-I at 5 W pump power.

In configuration-I, experiments were performed for both 976 nm and 906 nm to study the benefit of off-peak pumping. Almost similar spectral profile was observed for two wavelengths in Erbium band (Fig. 6a). Figure 6b shows spectra in 600–1100 nm band, under 976 nm pumping an appreciable peak at 1030 nm (parasitic lasing) appears in the output spectrum at ~ 6.8 W pump power. Besides the residual pump peak at 976 nm, visible radiation near 700 nm band was also observed that may be attributed to up-conversion from various excited levels of Erbium. Under 906 nm pumping, however, such prominent peaks were not observed even up to 7.5 W pump power. However, emission at ~ 976 nm may have resulted in parasitic lasing observed on silicon detector (given in following section). Such result is in contradiction to the earlier reported results [12, 13] for off-peak

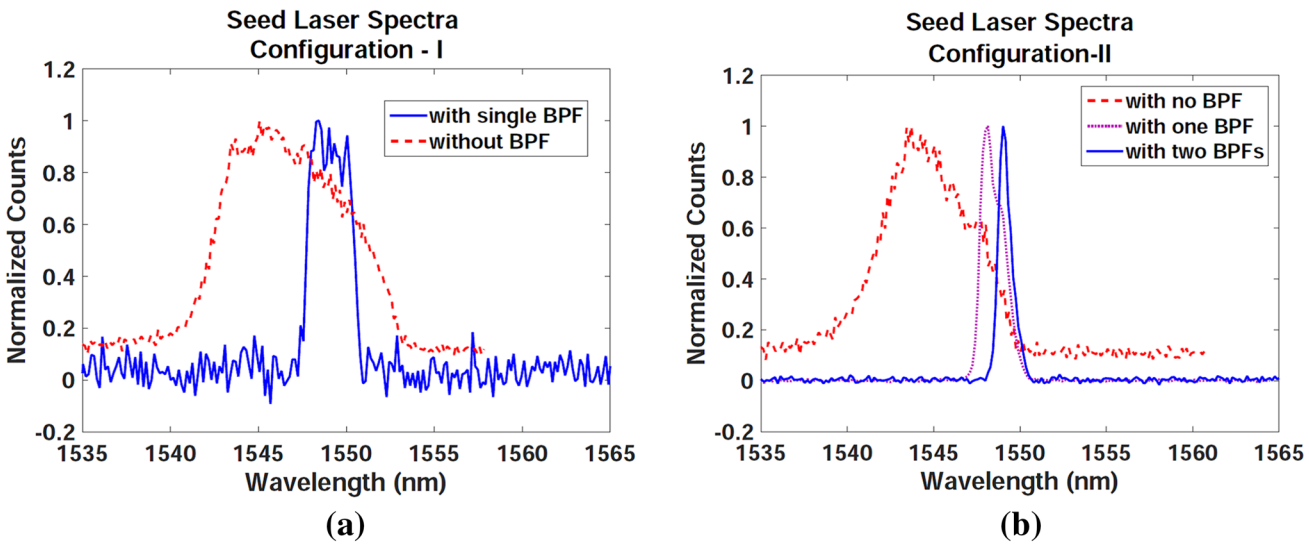

Fig. 4 Seed laser spectra **a** configuration-I, **b** configuration-II

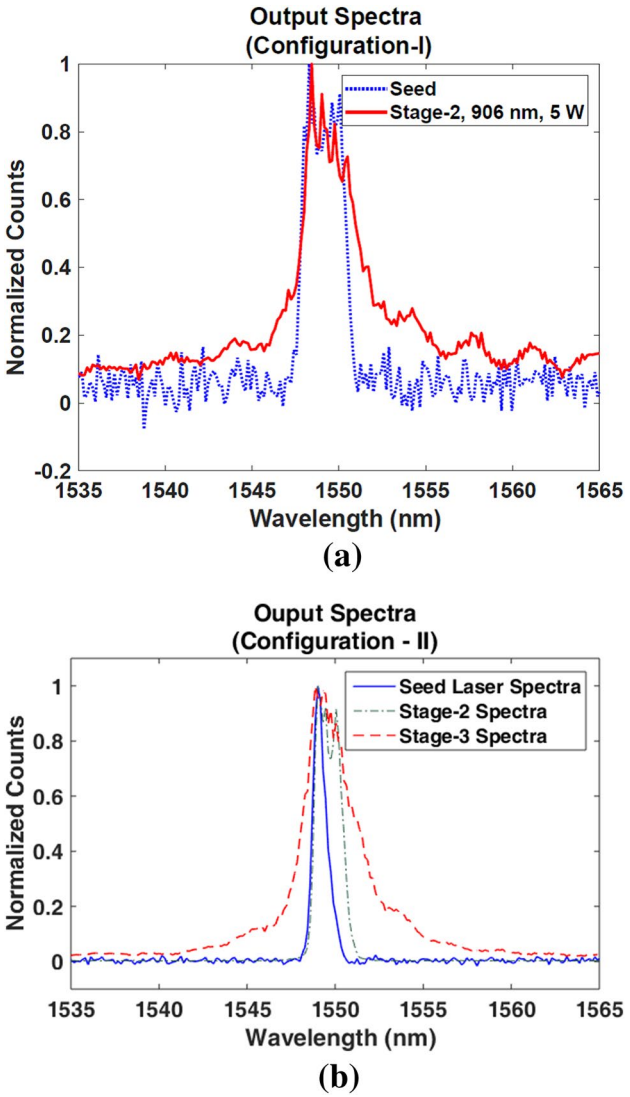

Fig. 5 Spectral overlap of various stages **a** configuration-I, **b** configuration-II for 906 nm pump

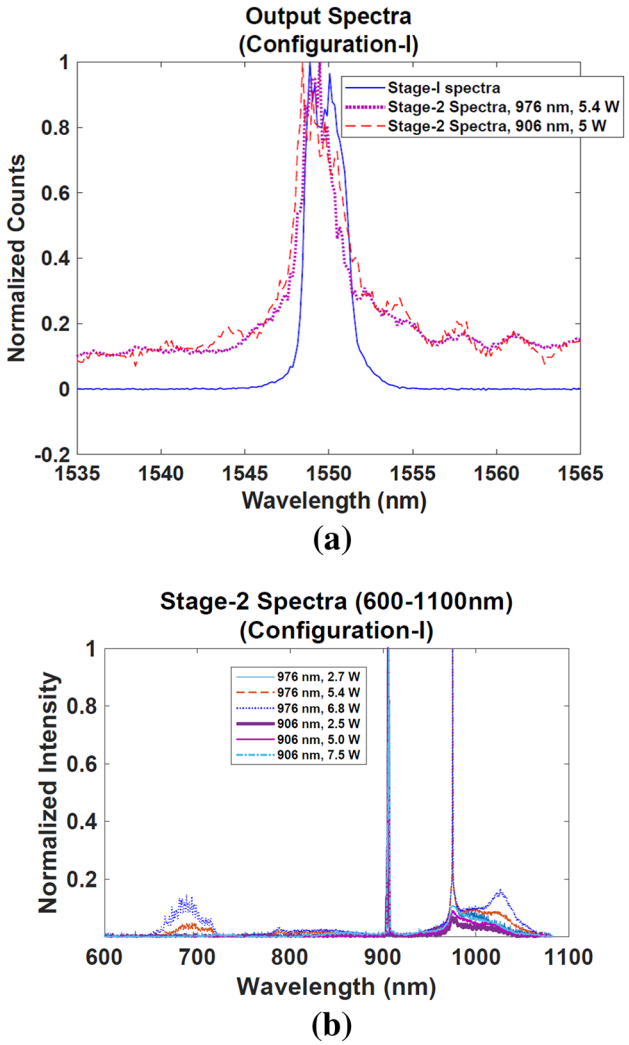

Fig. 6 Spectral overlap of various stages for both 906 nm and 976 nm pump in configuration-I. **a** In 1530–1560 nm band, **b** in 600–1100 nm band

pumping, where the spectrum was observed in 1–1.1 μm band and not below that.

3.2 Temporal performance

For detailed investigation of output pulses, we used both silicon and InGaAs photodetectors placed very close to the dichroic mirror in the corresponding arm, so that Yb parasitic lasing could be observed independent of in band ASE noise and self-pulsing. As the pump power increased, inter-pulse ASE started building up due to continuous pumping and near 5 W pump power, we could observe ns pulses, i.e. Yb parasitic lasing (Fig. 7) on the silicon detector just at the time of arrival of signal pulse.

As the pump power is increased further, prominent μs duration pulses start appearing during the off period. They resembled relaxation oscillations and to verify that we performed simple calculations of determining the time period of these oscillations at different pump powers (Fig. 8).

As per standard relaxation oscillation theory, if the gain built up in the signal OFF duration is sufficient to overcome the losses in the cavity, relaxation oscillations will initiate the lasing process. The frequency of the relaxation oscillations is determined by [28] the intra-cavity power P_{int}, the resonator losses l, the round-trip time T_{r} of the resonator, and the saturation energy E_{sat} and the upper-state lifetime τ_{g} of the gain medium:

$$f_{\text{ro}} = \frac{1}{2\pi}\sqrt{\frac{l}{T_{\text{r}}}\frac{P_{\text{int}}}{E_{\text{sat}}} - \frac{1}{4}\left[\frac{1}{\tau_{\text{g}}} + \frac{P_{\text{int}}}{E_{\text{sat}}}\right]^2}. \quad (1)$$

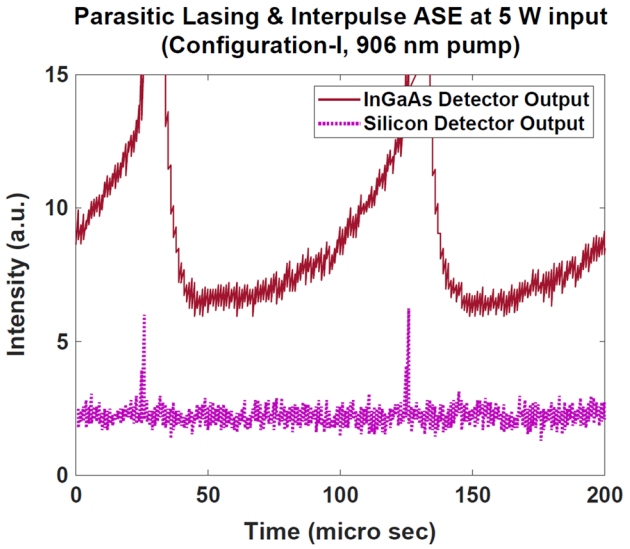

Fig. 7 Temporal profile at 5 W input

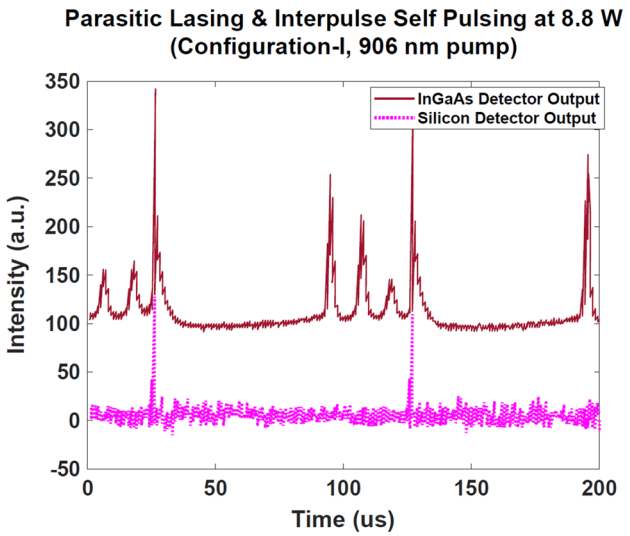

Fig. 8 Temporal profile at 8.8 W input

For Erbium (with $\tau_g >> T_r$), the second term of the radicand is negligible, so that the equation simplifies to

$$f_{ro} \approx \frac{1}{2\pi}\sqrt{\frac{l}{T_r}\frac{P_{int}}{E_{sat}}}. \tag{2}$$

In present case, the EYDF fiber has a core diameter of 12 µm with emission and absorption cross-section values as 1.73597E−25 m^2 and 1.16508E−25 m^2, respectively, at 1550 nm, leading to saturation energy value of 50 µJ using the following expression:

$$E_{sat} = \frac{Ah\nu}{\sigma_{em} + \sigma_{abs}}, \tag{3}$$

where $h\nu$ is the photon energy at the signal wavelength, σ_{em} and σ_{abs} are the emission and absorption cross-sections at the emission wavelength, and A is the mode area.

In (2), all the parameters except cavity losses are known. By measuring oscillation frequency experimentally (Fig. 9), we were able to fit our results for $l \sim 4\%$ (Table 1). Pump power was not increased beyond 8.8 W to avoid catastrophic damage to the components.

Thus, we conclude the origin of self-pulsing in our case is well explained by the relaxation oscillation theory.

Figure 10 shows no such self-pulsing and parasitic lasing in configuration-II for the same fiber length at 906 nm pump power up to 12 W, limited by power-handling capability of output isolator.

All the pulse profiles shown above are taken with photodetectors very close to the output ends (with suitable safety precautions) to observe these effects near the bottom of laser pulses. Actual laser output pulses were captured at much higher voltage scale on oscilloscope. Seed and final amplifier stage output pulses from configuration-II are depicted in Fig. 11, due to high gain of the fiber amplifier the leading edge of the final pulse becomes steeper in comparison to the seed laser pulse, the pulse width (FWHM) remaining the same as ~ 30 ns.

3.3 Comparative output energies

In configuration-I, we achieved 5.2 µJ energy at maximum input pump power of 900 mW in bidirectional pump scheme for the preamplifier stage corresponding to a gain

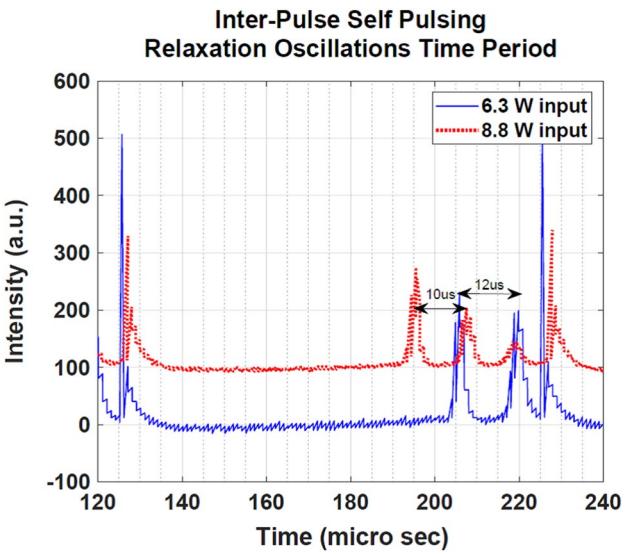

Fig. 9 Relaxation oscillations in configuration-I with 906 nm pump

Table 1 Comparison of theoretically estimated relaxation oscillation time period with experimental data

Loss	Length (m)	T_r (ns)	E_{sat} (μJ)	P_{int} (W)	f_{ro} (kHz)	T_{ro} (theoretical) (μs)	T_{ro} (experimental) (μs)
0.04	3.1	20.7	50	6.3	78.6	12.7	12
0.04	3.1	20.7	50	8.8	92.9	10.8	10

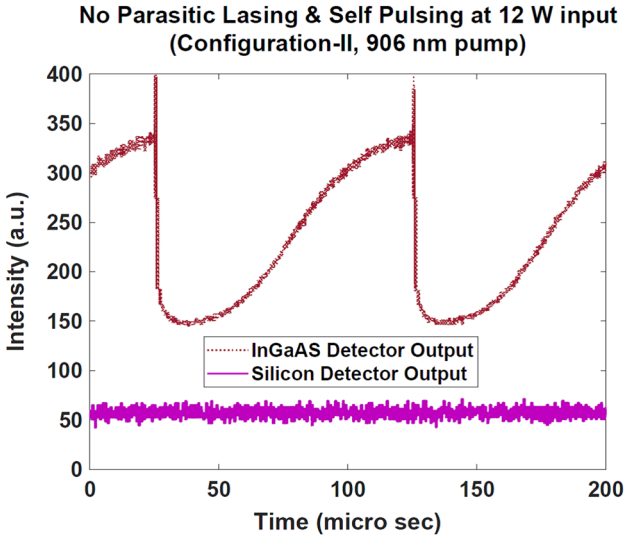

Fig. 10 Temporal profile in configuration-II at 12 W input

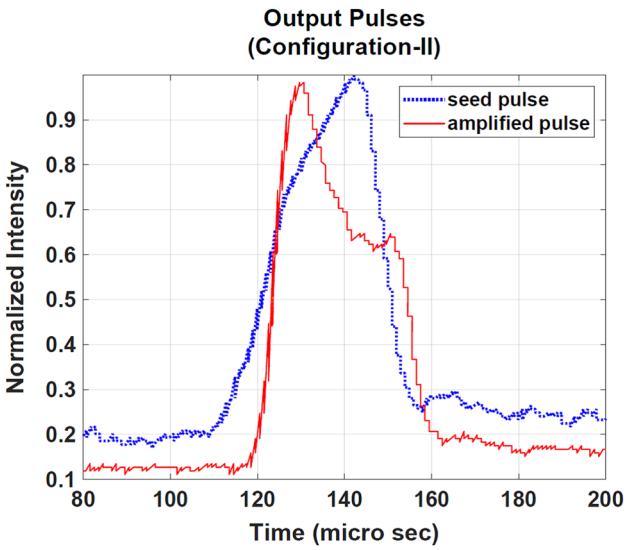

Fig. 11 Output pulse in configuration-II

of 28.7 dB, while in configuration-II, obtained 0.6 μJ (28.75 dB gain) from forward pumped first preamplifier and 2.5 μJ energy (6.2 dB gain) from second preamplifier, after two BPFs with total gain of 34.95 dB.

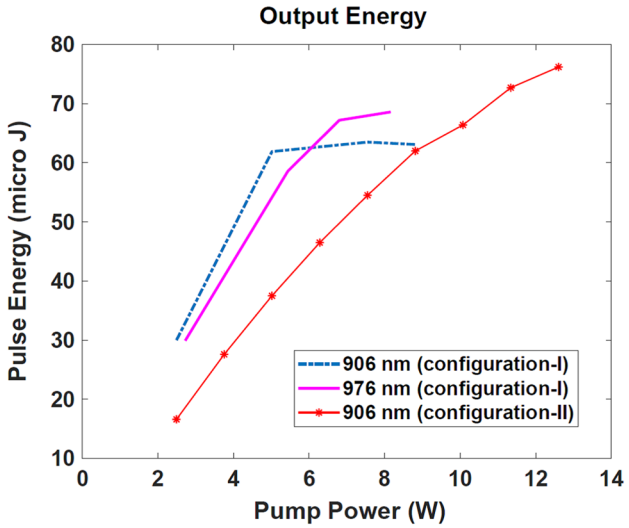

Fig. 12 Comparative output energies

For final amplifier stage (EYDF amplifier), measured output energies in two configurations are shown in Fig. 12. For 906 nm pump in configuration-I, a roll over in output energy (after ~ 60 μJ) is observed at ~ 5 W input power corresponding to the onset of Yb parasitic lasing (Fig. 7) which occurred much earlier than inter-pulse self-pulsing (Fig. 8). For 976 nm pump, output energy reaches a slightly higher value (68 μJ) at ~ 6.3 W and then got saturated. The better performance at 976 nm may be due to near optimum length (10 dB pump absorption) but for 906 nm, we avoided taking very long fiber (~ 5 m for 10 dB pump absorption) for increased threshold for non-linear (SRS) effect. However, in configuration-II with same fiber length for 906 nm pumping, the output energy was found to increase almost linearly up to 12 W input where more than 2.5 kW peak power (75 μJ energy per pulse of 30 ns duration) and 750 mW average power was achieved, limited by power-handling capability of output isolator.

Further optimization is under progress. We may continue to use 976 nm diodes for pumping EYDF fiber as the available diodes with us are wavelength stabilized also as per our experimental observations, not much significant advantage is expected at 906 nm (which is actually rated as 915 nm diode) even after length optimization. We plan to add suitable high-power BPF at the output of 12/130 amplifier stage to amplify

it further in another stage of 25/300 EYDF amplifier available commercially. Other parameters, e.g. beam quality (M^2 value) and polarization extinction ratio (P.E.R), shall be characterized after adding collimator at the final stage output of 25/300 EYDF fiber and results shall be reported in near future.

4 Conclusions

Extensive experiments carried out to improve the performance of an EYDF amplifier and generate 2.5 kW peak power laser pulses with 30 ns duration and 10 kHz repetition rate at 1.55 μm eye safe wavelength. In CW pumped pulsed fiber amplifier configuration, even 10 kHz repetition rate has found to be sufficiently low to give considerable time for inter-pulse ASE to build up. During no signal time (off period) at high pump powers, self-pulsing may get triggered which may cause damage to various components. Also due to co-doping of Ytterbium ions, parasitic lasing in Yb emission band is also inevitable. In the presence of these effects, situation may arise when with increasing pump input no increase or fall in output energy and average power is observed. We have presented here several novel experimental results in terms of spectral, temporal and energy output for a pulsed EYDF amplifier operating at 30 ns, 10 kHz and generating 2.5 kW pulses @ 1550 nm. First of all, a cost-effective directly modulated broadband Fabry–Perot laser diode has been employed as a seed rather than a DFB diode with extremely narrow linewidth, which may not be suitable for certain applications like speckle free imaging.

Second, with a very simple scheme of adding two BPFs in tandem after seed and second preamplifier stage, we have been able to suppress the Yb parasitic lasing and inter-pulse self-pulsing, thus avoided complex gating and pulsed pumping schemes up to 12 W pump power levels. Third, result pertains to the off-pumping at 906 nm, where we could not get much advantage, as Yb parasitic lasing was observed near 976 nm instead of 1000–1100 nm spectral range at much lower power level of 5 W than for 976 nm pumping. Fourth and last, finding is related to the self-pulsing origin, which in our case is well explained by relaxation oscillation theory. Theoretically calculated time period (10–12 μs) of the self-pulses at various pump powers matched fairly well with the experimental results. Comparative results have been presented for two different MOPA configurations. MOPA with broader signal spectrum resulted in Yb parasitic lasing at 5 W pump power causing roll over in the output energy. Also, onset of strong self-pulsing was observed during off period (in absence of signal pulse) at ~ 6.3 W input. Nature of these pulses resembled relaxation oscillations. In configuration-II with reduced ASE noise, output energy could be scaled up by 25%. Maximum pulse energy of 75 μJ at 10 kHz corresponding to 750 mW average power output at 12 W pump input could be achieved from a double clad Nufern make PM 12/130 EYDF fiber. It is planned to add another amplifier stage to reach up to 1 mJ per pulse in near future.

Acknowledgements Authors are extremely thankful to Director, LASTEC for providing permission to pursue this work using Pulsed Laser Sources (PLS) lab facilities. Technical support from Atul Bhardwaj of PLS group, LASTEC, is also highly acknowledged.

References

1. Y. Jeong, S. Yoo, C.A. Codemard, J. Nilsson, J.K. Sahu, D.N. Payne, R. Horley, P.W. Turner, L. Hickey, A. Harker, M. Lovelady, A. Piper, IEEE J. Sel. Top. Quantum Electron. **13**, 573 (2007)
2. V. Kuhn, P. Weßels, J. Neumann, D. Kracht, Opt. Express **17**, 18304 (2009)
3. V. Kuhn, D. Kracht, J. Neumann, P. Weßels, Opt. Lett. **35**, 4105 (2010)
4. Q. Han, J. Ning, Z. Sheng, IEEE J. Quantum Electron. **46**, 1535 (2010)
5. Q. Han, Y. He, Z. Sheng, W. Zhang, J. Ning, H. Xiao, Opt. Lett. **36**, 1599 (2011)
6. G. Sobon, P. Kaczmarek, A. Antonczak, J. Sotor, K.M. Abramski, Opt. Express **19**, 19104 (2011)
7. G. Sobon, D. Sliwinska, P. Kaczmarek, K.M. Abramski, Opt. Commun. **285**, 3816 (2012)
8. X. Zhao, Q. Han, D. Wang, H. Hu, K. Ren, J. Jiang, T. Liu, Opt. Lett. **44**, 1100 (2019)
9. D. Ouyang, C. Guo, S. Ruan, P. Yan, H. Wei, J. Luo, Appl. Phys. B Lasers Opt. **114**, 585 (2014)
10. M. Klopfer, M.K. Block, J. Deffenbaugh, Z.G. Fitzpatrick, M.T. Urioste, L.J. Henry, R. Jain, in *Laser Resonators, Microresonators, and Beam Control XIX*, ed. by A. V. Kudryashov, A. H. Paxton, and V. S. Ilchenko (2017), p. 100901N
11. I. Pavlov, E. Dülgergil, E. Ilbey, F.Ö. Ilday, Opt. Lett. **39**, 2695 (2014)
12. D.J. Creeden, J.R. Limongelli, H.S. Pretorius, S.D. Setzler, US Patent No. 9620,924 B1 (2017)
13. M. Steinke, H. Tunnermann, V. Kuhn, T. Theeg, M. Karow, O. De Varona, P. Jahn, P. Booker, J. Neumann, P. Wesels, D. Kracht, IEEE J. Sel. Top. Quantum Electron. **24**, 1–3 (2018)
14. R. Rangel-Rojo, M. Mohebi, Opt. Commun. **137**, 98 (1997)
15. N. Li, Purnawirman, J.D. Bradley, G. Singh, E.S. Magden, J. Sun, M.R. Watts, in *2015 Optoelectronics Global Conference (OGC)*, IEEE (2015), pp. 1–2
16. S. Sergeyev, K. O'Mahoney, S. Popov, A.T. Friberg, Cent. Eur. J. Phys. **8**, 159 (2010)
17. E. Lacot, F. Stoeckel, M. Chenevier, Phys. Rev. A **49**, 3997 (1994)
18. F. Sanchez, G. Stephan, Phys. Rev. E **53**, 2110 (1996)
19. S.V. Sergeyev, Opt. Lett. **41**, 4700 (2016)
20. A.-R. Sterian and V. Ninulescu, in *Proceedings of SPIE—The International Society for Optical Engineering*, ed. by P.A. Atanasov, S.V. Gateva, L.A. Avramov, A.A. Serafetinides (2005), p. 551
21. O. de Varona, W. Fittkau, P. Booker, T. Theeg, M. Steinke, D. Kracht, J. Neumann, P. Wessels, J.L. Wagener, P.F. Wysocki, M.J.F. Digonnet, H.J. Shaw, D.J. DiGiovanni, M. Steinke, A. Croteau, C. Paré, H. Zheng, P. Lampere, A. Proulx, J. Neumann, D. Kracht, P. Wessels, C. Er, Opt. Lett. **18**, 2014 (1993)

22. P.-H. Hanzard, M. Talbi, D. Mallek, A. Kellou, H. Leblond, F. Sanchez, T. Godin, A. Hideur, Sci. Rep. **7**, 45868 (2017)
23. W.H. Loh, J.P. de Sandro, Opt. Lett. **21**, 1475 (1996)
24. H. Chen, G. Zhu, N.K. Dutta, K. Dreyer, Appl. Opt. **41**, 3511 (2002)
25. L. Luo, P.L. Chu, Opt. Lett. **22**, 1174 (1997)
26. D. Amroun, A. Kellou, K.A. Ameur, V. Dupray, F. Sanchez, J. Mod. Opt. **47**, 1247 (2000)
27. M. Ding, P.K. Cheo, IEEE Photonics Technol. Lett. **9**, 324 (1997)
28. A.E. Siegman, *Lasers* (University Science Books, Mill Valley, 1986)
29. J.W. Dawson, M.J. Messerly, R.J. Beach, M.Y. Shverdin, E.A. Stappaerts, A.K. Sridharan, P.H. Pax, J.E. Heebner, C.W. Siders, C.P.J. Barty, Opt. Express **16**, 13240 (2008)